

# Tomographically normal partner eye in very asymmetrical corneal ectasia: biomechanical analysis



Doris Fraenkel, MD, Loïc Hamon, MD, Loay Daas, MD, Elias Flockerzi, MD, Shady Suffo, MD, Timo Eppig, PhD, Berthold Seitz, MD, ML, FEBO

**Purpose:** To point out the biomechanical changes of the topographically and tomographically normal partner eye (NPE) in patients with very asymmetrical corneal ectasia.

**Setting:** Department of Ophthalmology, Saarland University Medical Center in Homburg/Saar, Germany.

**Design:** Retrospective study.

**Methods:** The topographical and tomographical results of the NPE were assessed using the Pentacam HR and the biomechanical corneal properties using the Ocular Response Analyzer (keratoconus match index [KMI], corneal hysteresis [CH], and corneal resistance factor [CRF]) and the Corvis ST (topographic biomechanical index [TBI] and Corvis biomechanical index) and compared those results with a normal control group (CG).

**Results:** The clinical records of 26 patients recruited from the Homburg Keratoconus Center diagnosed with a very asymmetrical

corneal ectasia were reviewed. The NPE ( $8.5 \pm 1.5$  mm Hg) showed a significantly more pathological CH ( $P < .001$ ) compared with the CG. The CRF was also significantly more pathological ( $P = .04$ ) for the NPE ( $8.3 \pm 1.5$  mm Hg) compared with the CG. The NPE ( $0.62 \pm 0.32$ ) showed a nonsignificant ( $P = .08$ ) more pathological KMI compared with the CG. Nineteen (73.1%) of 26 NPE had a KMI less than 0.72 and were considered pathological. Compared with the CG, the TBI of the NPE ( $0.19 \pm 0.25$ ) did not differ significantly overall ( $P = .57$ ). However, 5 (19.2%) of 26 eyes had a TBI more than 0.29 and were considered pathological.

**Conclusions:** Topographically and tomographically NPEs in very asymmetrical corneal ectasia frequently showed biomechanical changes. This should be considered before planning any type of refractive corneal surgery in such patients.

*J Cataract Refract Surg* 2021; 47:366–372 Copyright © 2021 Published by Wolters Kluwer on behalf of ASCRS and ESCRS

**K**eratoconus is a degenerative, progressive corneal ectasia with an incidence varying from 3 to 2.340/100 000, depending on ethnicity and region.<sup>1</sup> The age of onset is typically during puberty and progresses until the third to fourth decade of life, when it tends to stabilize. The disorder is usually diagnosed during the second decade of life and is characterized by progressive corneal thinning and steepening, leading to the remodeling of the cornea into a conical shape.<sup>2,3</sup> This comes along with an irregular astigmatism and finally corneal scars, which result in a gradual decline of the corrected visual acuity.

The exact etiopathogenesis of keratoconus and its underlying biomechanical processes remain unclear, but both genetic and environmental factors have been associated with the disease.<sup>4–8</sup> Several studies have reported a

significantly increased incidence in certain ethnicities such as North-Pakistani, Iranian, and Saudi Arabian.<sup>9,10</sup> Keratoconus has also been linked with genetic disorders, such as Down syndrome, Leber congenital amaurosis, Ehlers-Danlos syndrome, osteogenesis imperfecta, and other connective tissue disorders. Those are clearly suggesting a genetic component to the disease.<sup>5</sup> Nevertheless, the genetic factors are multifactorial, and no conclusive genetic link has been established so far. Environmental factors, such as excessive eye rubbing, have also been proven to play a key role in the physiopathology of the disease.<sup>11–13</sup>

Keratoconus is usually bilateral but typically affecting both eyes with an asymmetrical severity, creating in some rare cases the feature of unilateral keratoconus.<sup>14</sup> However, several recent studies have been suggesting that true

Submitted: March 24, 2020 | Final revision submitted: August 15, 2020 | Accepted: August 24, 2020

From the Department of Ophthalmology, Saarland University Medical Center UKS (Fraenkel, Hamon, Daas, Flockerzi, Suffo, Seitz), and Institute of Experimental Ophthalmology, Saarland University (Eppig), Homburg/Saar, and AMIPLANT GmbH (Eppig), Schnaittach, Germany.

D. Fraenkel and L. Hamon contributed equally to this work.

Presented at the ARVO Annual Meeting, Vancouver, Canada, May 2019, and SFO International Congress, Paris, France, May 2019.

Corresponding author: Doris Fraenkel, MD, Department of Ophthalmology, Saarland University Medical Center UKS, Kirrbergerstraße 100, Bldg 22, 66421 Homburg/Saar, Germany. Email: [doris.fraenkel@uks.eu](mailto:doris.fraenkel@uks.eu).

unilateral keratoconus does not exist, showing a prevalence between 0.5% and 4%.<sup>1,2</sup> It is important to differentiate unilateral keratoconus from the early subclinical form of the disease, forme fruste keratoconus, already presenting topographical and tomographical pathological changes but insufficient to reach the threshold of keratoconus, based on computed quantitative indices.<sup>15,16</sup> On the contrary, the normal partner eye in unilateral keratoconus or very asymmetric ectasia shows no clinical or topotomographical changes. Studies still debate the right nomenclature and struggle to define the right criteria for defining abnormal tomography. Even though recent studies suggest that true unilateral keratoconus does not exist, there are some cases of pure unilateral ectasia caused by environmental triggers, such as ocular trauma, rigid contact lenses wear, or ocular surgery.<sup>17</sup>

Modern advances in computer-assisted technologies and imaging techniques have increased our ability to analyze and diagnose preclinical stages of the disease. They represent sensitive means for detecting subtle changes of the topography on the corneal surface.<sup>2</sup> Recent studies have shown that biomechanical destabilization of the cornea in keratoconic eyes (KEs) might be present before topographical changes, and it might be detectable prior to the tomographic and clinical signs of the disease.<sup>18</sup> However, the early diagnosis of its subclinical forms still represents a daily challenge. Unfortunately, unknown subclinical forms still undergo refractive corneal surgery such as laser in situ keratomileusis (LASIK), which is a clear contraindication. Furthermore, severe ectatic corneal disorders were reported after LASIK in patients with no previous findings of corneal abnormalities.<sup>19,20</sup> The purpose of this study was to point out the biomechanical changes of the topographically and tomographically normal partner eye (NPE) in patients with very asymmetrical corneal ectasia.

## METHODS

This retrospective study was conducted at the Department of Ophthalmology, Saarland University Medical Center in Homburg/Saar, Germany. The study and data acquisition were performed with approval from the ethics committee of the Saarland Medical Association (Ethik-Kommission der Ärztekammer des Saarlandes, Nr. 157/10). The study adhered to the tenets of the Declaration of Helsinki.

The clinical records of 1730 patients from the Homburg Keratoconus Center were collected and reviewed.<sup>1</sup> Twenty-six patients (1.5%) were diagnosed with a very asymmetrical corneal ectasia and were recruited.

First, the data were divided into 3 groups (Table 1). The clinically, topotomographically, and biomechanically clearly pathological eyes (KE) (group 1) were compared with the

clinically, topographically, and topographically NPE (group 2). For the normal control group (CG) (group 3), the clinical records of 25 coworkers (50 eyes) from Department of Ophthalmology, without any clinical evidence or family history of corneal ectasia and without any corneal abnormalities or history of corneal surgery, were used. The CG showed no clinical and topographical abnormalities. Patients with ocular surgery history or accompanying ocular pathology were excluded from the study. The biomechanical properties of 16 patients (31 eyes) who underwent LASIK with a follow-up of at least 2 years was analyzed, showing no evidence of post-LASIK ectasia into a LASIK control subgroup.

All patients underwent a complete clinical, topographical and tomographical, and biomechanical examination. The Pentacam HR (OCULUS Optikgeräte GmbH) was used for generating a Scheimpflug corneal topography with images of the anterior and posterior surface topography of the cornea. The anterior astigmatism, the power of the flatter axis on the anterior surface of the cornea at 3.2 mm (K1), the power of the steeper axis on the anterior surface of the cornea at 3.2 mm (K2), the power of the steeper axis on the anterior surface of the cornea (Kmax), and the thinnest corneal thickness (TCT) were analyzed. The Pentacam also provided a series of keratoconus-specific indices: index of surface variance (ISV), index of height asymmetry (IHA), index of height decentration (IHD), index of vertical asymmetry (IVA), keratoconus index (KI), and central keratoconus index (CKI).<sup>21</sup> The Pentacam random forest index (PRFI) and the Belin/Ambrosio display enhanced ectasia total derivation value (BAD-D) were also included.<sup>22,23</sup>

The biomechanical corneal properties were analyzed using the Ocular Response Analyzer (ORA) (Reichert Ophthalmic Instruments) and the Oculus Corvis ST (OCULUS Optikgeräte GmbH). The ORA provides 2 keratoconus-specific indices, the keratoconus match probability (KMP) and the keratoconus match index (KMI). The cutoff value for typically subclinical keratoconus was defined as less than 0.72 for KMI, which represents the point between nonectatic corneas (0.94) and keratoconus stage 1 corneas (0.46), according to the Amsler-Krumeich criteria.<sup>15</sup> The corneal hysteresis (CH) and corneal resistance factor (CRF), 2 measures of the corneal rigidity provided by the ORA, were also analyzed. The cutoff value for keratoconus is defined as less than 9.9 mm Hg for CH and less than 8.8 mm Hg for CRF.<sup>24</sup> The OCULUS Corvis ST produced various biomechanical parameters (stiffness A1 [SP-A1], integrated ratio [IR], Ambrósio's relational thickness to the horizontal profile [ARTh], and deformation amplitude ratio [DA-ratio]). Two indices are then generated, the Corvis biomechanical index (CBI) and tomographic biomechanical index (TBI). The cutoff value for keratoconus is defined as more than 0.29 for TBI and more than 0.5 for CBI.<sup>23,25</sup>

The criteria for normal condition and disease were based on a collective assessment of refraction examination, slitlamp anterior segment examination (corneal stromal thinning, Fleischer ring, Vogt striae, and subepithelial scars), and Pentacam HR.<sup>2</sup> The diagnosis of very asymmetric ectasia was made when one eye was clearly pathological and the partner eye did not present any clinical or topographical and tomographical signs of corneal abnormalities, including the posterior corneal surface with a change in elevation (posterior

**Table 1. Demographic characteristics.**

Characteristic	Group 1, KE	Group 2, NPE	Group 3, CG	Group 4, CGL
Patients, n, sex	26 (17M, 9F)	26 (17M, 9F)	25 (7M, 18 F)	16 (11M, 5 F)
Eyes, n, sex	26 (17M, 9F)	26 (17M, 9F)	50 (14M, 36 F)	31 (21M, 10F)
Age (y) mean ± SD	33.6 ± 13.3	33.6 ± 13.3	35.7 ± 8.3	38.5 ± 12.4

CG = control group; CGL = control group laser in situ keratomileusis; F, female sex; KE = keratoconic eyes; M, male sex; NPE = topotomographically normal partner eyes

elevation difference [PED]) (from the baseline to the exclusion map) of 12  $\mu\text{m}$  or less (back elevation map and BAD-D).<sup>26</sup> The criteria for normality was defined as follows: no clinical signs of corneal ectasia, TCT of 506.5  $\mu\text{m}$  or lesser, Kmax of 42.5 diopter (D) or lesser, KI of 1.04 or lesser, IHA of 12.5 or lesser, IHD of 0.0205 or lesser, ISV of 32.5 or lesser, IVA of 0.240 or lesser, Rmin of 7.320 mm or greater, and PED of 12  $\mu\text{m}$  or lesser.<sup>22,26–30</sup>

### Statistical Analysis and Methods

The mean of the values for each group for the topotomographical parameters (K1, K2, Kmax, astigmatism, TCT, ISV, IHA, IHD, IVA, KI, CKI, BAD-D, and PRFI) and for each biomechanical parameter (KMI, CH, CRF, CBI, TBI, SP-A1, IR, ARTh, and DA-ratio) were calculated. The standard deviation (SD) to quantify the amount of variation of the data values for each group and for all the parameters was calculated.

A Kruskal-Wallis test with Bonferroni adjustment for small cohorts and multiple comparisons was used to compare the NPE group and the CG for each parameter. The results were described as a probability value ( $P$ ) with a CI of 95% (2-tailed). The Cohen effect sizes for the samples to measure whether the 2 groups have similar standard deviations and are of the same size and thereby assuring the strength of the statistical claim were also calculated. Cohen reports the following intervals for interpreting the magnitude of effect size: 0.1 to 0.3, small effect; 0.3 to 0.5, intermediate effect; and 0.5 and higher, strong effect.<sup>31</sup>

Receiver operating characteristic (ROC) curves were applied to determine the overall predictive accuracy of the CH, CRF, CBI, KMI, and TBI to detect signs of corneal ectasia on the NPE, as described by the area under the curve (AUC). ROC curves are obtained by plotting sensitivity vs (1 – specificity), which are calculated for each value observed. An area of 100% implies that the test perfectly differentiates between the study groups. All the statistical analysis was performed with SPSS Statistics for Windows software (SPSS, Inc.).

### RESULTS

The results of the 26 patients are summarized in Tables 1 and 2 (see Supplemental Digital Content 1, available at <http://links.lww.com/JRS/A215>). The corneal topography, using the Pentacam HR, showed that the KE had highly pathological results, as expected. All the following parameters of the Pentacam HR: K1, K2, Kmax, astigmatism, TCT, ISV, IHA, IHD, IVA, KI, CKI, BAD-D, and PRFI, showed pathological results, which are high above the defined cutoff for keratoconus. The NPE group along with the CG presented similar results, showing no signs of topographical abnormalities, as expected (Figure 1). Compared with the CG (10.6  $\pm$  1.8 mm Hg, min: 7.5 max: 14.4), the NPE group (8.5  $\pm$  1.5 mm Hg, min: 5.1 max: 11.5) showed a significantly more pathological CH (Cohen effect size = 1.23;  $P < .001$ ). In comparison with the CG (9.8  $\pm$  2.1 mm Hg, min: 5.8 max: 14.5), the CRF was also significantly more pathological (Cohen effect size = 0.8;  $P = .04$ ) for the NPE group (8.3  $\pm$  1.5 mm Hg, min: 5.8 max: 11.1). CH and CRF did not show any significant difference between the KE and the NPE groups ( $P = .73$  and  $P = .1$ , respectively).

Compared with the CG (0.84  $\pm$  0.33, min: 0.14 max: 1.56), the NPE group (0.62  $\pm$  0.32, min: 0.09 max: 1.35) showed no significantly more pathological KMI (Cohen effect size = 0.68;  $P = .08$ ) (Figure 2). However, 19 (73.1%)

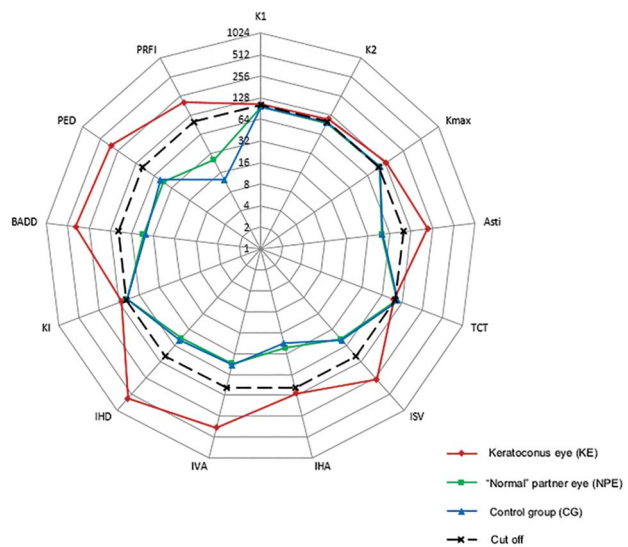


**Figure 1.** Parameters of the Scheimpflug camera for the detection of keratoconus (in percentage of pathological value). Representation of the topographical and tomographical values and indices for the KE group, NPE group, and CG. The *black line* represents the pathological cutoff point for corneal ectasia, which differ for each parameter. All values are represented in a percentage of these cutoff values, logarithmically scaled. Values more than 100% (outside the *cutoff line*) are pathological, except for the TCT, where the pathological values are inside the line. The values of the KE group are clearly above the cutoff for most of the parameters. The values of the NPE groups and CG are under the cutoff points and are very similar (except for PRFI) (Asti = astigmatism; BAD-D = Belin/Ambrosio display enhanced ectasia total derivation value; CG = control group; IHA = index of height asymmetry; IHD = index of height decentration; ISV = index of surface variance; IVA = index of vertical asymmetry; K1 = flat keratometry; K2 = steep keratometry; KE = keratoconic eye; KI = keratoconus index; Kmax = maximum keratometry; NPE = topotomographically normal partner eye; PRFI = Pentacam Random Forest Index; TCT = thinnest corneal thickness).

of the 26 NPE had a KMI less than 0.72 and were, therefore, considered to be pathological.

Compared with the CG (0.08  $\pm$  0.11, min: 0.00 max: 0.40), the TBI of the NPE group (0.19  $\pm$  0.25, min: 0.0 max: 0.99) did not differ statistically significantly overall (Cohen effect size = 0.62;  $P = .57$ ). However, 5 (19.2%) of the 26 patients with NPE had a TBI more than 0.29 and were, thus, considered to be pathological (Figure 3).

In comparison with the CG (0.25  $\pm$  0.27, min: 0.00 max: 1.00), the CBI of the NPE group (0.07  $\pm$  0.16, min: 0.00 max: 0.62) was significantly less pathological, meaning that the CBI of the CG was closer to the CBI of the KE compared with the NPE (Cohen effect size = 0.85;  $P = .02$ ). Nevertheless, 2 (7.7%) of 26 patients with NPE had a CBI more than 0.50 and were, therefore, considered pathological (Figure 4). The biomechanical parameters (ARTh, SP-A1, DA-ratio, and IR) measured with the Corvis ST were analyzed individually. However, compared with the CG, the NPE group showed no significant difference (Table 2).

The CGL (stable patients who underwent LASIK) showed significantly different values compared with the CG, with a CH of 9.8  $\pm$  1.6 mm Hg (difference between CG and CGL:  $P = .13$ ), a CRF of 8.9  $\pm$  1.9 mm Hg ( $P < .001$ ), a

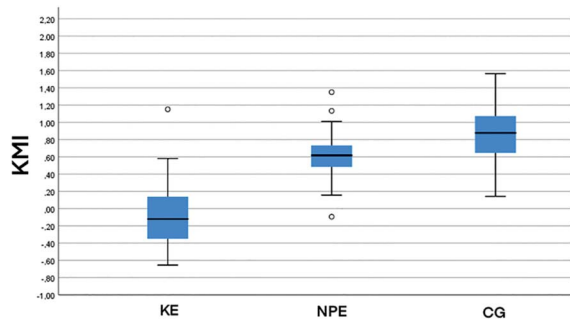


Figure 2. Keratoconus match index (KMI) (CG = control group; KE = keratoconic eye; NPE = topo-tomographically normal partner eye).

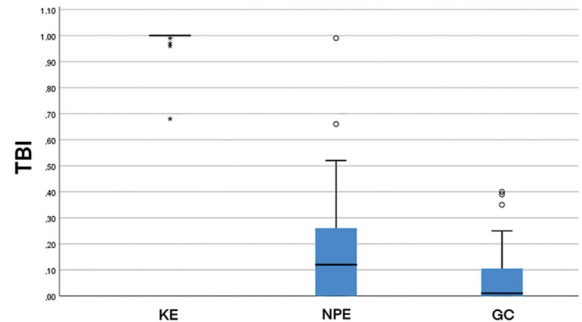


Figure 3. Tomographic biomechanical index (TBI) (CG = control group; KE = keratoconic eye; NPE = topotomographically normal partner eye).

KMI of  $0.60 \pm 0.32$  ( $P = .004$ ), a TBI of  $0.58 \pm 0.37$  ( $P < .001$ ), and a CBI of  $0.51 \pm 0.41$  ( $P = .023$ ).

In comparison with the KMI and CBI, the TBI showed a poor ability to detect biomechanical changes on the NPE (AUC = 0.35, standard error [SE] = 0.075). The CH showed the best ability to detect biomechanical abnormalities (AUC = 0.76, SE = 0.061), followed by the CBI (AUC = 0.74, SE = 0.063), the KMI (AUC = 0.68, SE = 0.07), and the CRF (AUC = 0.65, SE = 0.069) (Figure 5).

**DISCUSSION**

Because keratoconus is known to affect the biomechanical corneal stability, it should also be possible to be diagnosed based on instruments with the ability to measure the corneal biomechanical properties, such as the ORA or OCULUS Corvis ST.

In 2005, Reichert Ophthalmic Instruments introduced the ORA as the first reliable noncontact pneumotonometer, measuring the corneal biomechanical response in vivo. The ORA measures aspects of the corneal biomechanical response during an air-puff perturbation, such as height, slope, and width of the deformation’s dynamics.<sup>23</sup> These so-called waveform parameters represent the ophthalmic viscosurgical device damping capabilities and overall elastic resistance of the cornea and are displayed in a waveform signal. The CH represents the cornea’s ability to absorb and dissipate energy. It describes the difference in the inward and outward pressure values obtained during the patented dynamic bidirectional applanation process of the ORA. The

CRF is the same measurement, corrected with a k value integrating the central corneal thickness, making the measure independent to the intraocular pressure.<sup>24</sup>

The updated software version (3.0) of the ORA also provides 2 new keratoconus-specific indices, the KMI and KMP. These are the mathematical representations of waveform shape characteristics of the analyzer. Considering certain ocular pathologies are supposed to share common waveform patterns, theoretically, they could be classified according to their biomechanical properties. The KMI (including 7 parameters) represents the similarity of the waveform of an eye to the average waveform characteristics of various keratoconus eyes. The KMP attempts to demonstrate how the given measurement matches the reference population data. It represents the probability that a cornea is normal, suspect, or ectatic and classifies the measurement as potentially normal, suspect, mild, moderate, or severe keratoconus.<sup>32</sup> As previously mentioned, the cutoff value for typical subclinical keratoconus is defined as less than 0.72 for KMI, which represents the point between nonectatic corneas (0.94) and keratoconus stage 1 corneas (0.46), according to the Amsler-Krumeich criteria.<sup>15</sup>

Numerous studies have attempted to explore the diagnostic capacity of the ORA about detecting keratoconus and keratoconus-suspect eyes.<sup>33–36</sup> Shah et al. compared the CH in normal eye and KEs using the ORA. The study showed that the CH was significantly higher in normal eyes than that in KEs and, thus, concluded that the ORA might be useful to assess the progression of the disease because hysteresis might change even before topographic or clinical changes become apparent.<sup>33</sup>

In 2013, Labiris et al. attempted to evaluate the diagnostic capacity of the ORA in keratoconus-suspect eyes. They compared keratoconus-suspect eyes with healthy eyes with the ORA using the KMI and KMP indices. They found that the KMI differed significantly between control eyes and keratoconus-suspect eyes with an overall predictive accuracy of 94% (cutoff point 0.72). The KMP index, on the other hand, showed limited diagnostic value, because it insufficiently differentiated between keratoconus-suspect corneas and normal corneas. A high percentage of suspect eyes in the normal population and a high percentage of KMP-derived normal eyes in the keratoconus-suspect

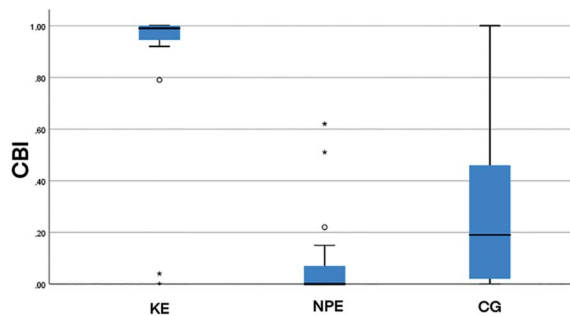


Figure 4. Corvis biomechanical index (CBI) (CG = control group; KE = keratoconic eye; NPE = topo-tomographically normal partner eye).

**Table 2. Statistical analysis of the parameters for the 3 main groups.**

	Group 1, KE (n = 26)	Group 2, NPE (n = 26)	Group 3, CG (n = 50)	Comparison Between Groups 2 and 3
	Mean ± SD	Mean ± SD	Mean ± SD	P Value <sup>‡,§</sup>
CH	7.9 ± 1.9	8.5 ± 1.5	10.6 ± 1.8	<.001*
CRF	6.9 ± 2.0	8.3 ± 1.5	9.8 ± 2.1	.04*
KMI	-0.05 ± 0.4	0.62 ± 0.32	0.84 ± 0.33	.08
TBI	0.98 ± 0.1	0.19 ± 0.25	0.08 ± 0.11	.57
CBI	0.89 ± 0.27	0.07 ± 0.16	0.25 ± 0.27	.02 <sup>†</sup>
SP-A1	73.8 ± 21.9	96.1 ± 12.7	101.5 ± 15.9	.77
IR	11.1 ± 2.6	7.8 ± 0.8	7.6 ± 0.9	1
ARTh	244.7 ± 146.1	512 ± 88.3	484.3 ± 107.4	.77
DA-ratio	5.3 ± 1.16	4.2 ± 0.4	4.2 ± 0.4	1

ARTh = Ambrósio's relational thickness to the horizontal profile; CBI = Corvis biomechanical index; CH = corneal hysteresis; CRF = corneal resistance factor; DA-ratio = deformation amplitude ratio; IR = integrated ratio; KMI = keratoconus match index; SP-A1 = stiffness parameter A1; TBI = topographic biomechanical index

\* $P < .05$ ; NPE is significantly more pathological than CG.

<sup>†</sup> $P < .05$ ; NPE is significantly less pathological than CG.

<sup>‡</sup>2-tailed test.

<sup>§</sup>Statistical probability calculated with a Kruskal-Wallis test with Bonferroni adjustment for multiple comparisons that the difference between the values for the NPE group and the CG is randomly linked and cannot be explained by the hypothesis.

group were found. They concluded that this high percentage of suspect eyes in the normal population reflects an insufficiency of the index that limits its clinical value in differentiating keratoconus-suspect corneas from normal corneas.<sup>34</sup>

The OCULUS Corvis ST is a new-generation noncontact tonometer recording the corneal biomechanical response to a collimated air pulse using a high-speed Scheimpflug camera to monitor corneal deformation. The system generates and analyzes various biomechanical parameters: SP-A1, the resulting pressure at inward applanation (A1) divided by the corneal displacement; IR, the AUC of the inverse of radius (1/R) in function of time for the central radius of curvature during the concave phase of corneal deformation; ARTh, an index based on the thickness profile in the temporal–nasal direction; DA-ratio, the ratio between the DA (vertical displacement) at the corneal apex and the DA at 1.0 or 2.0 mm nasal and temporal from the apex.<sup>21</sup> Those are compared with a normative database. The CBI and TBI are 2 indices calculated with the aforementioned parameters with the purpose of early detection of subclinical corneal ectasia such as keratoconus. The TBI combines the tomographic and biomechanical parameters to reach maximal accuracy.<sup>21,23,25</sup>

In 2017, Vinciguerra et al. investigated the capability of the Corvis ST to diagnose early corneal ectasia. They found biomechanical abnormalities, whereas tomography and topography were normal.<sup>37</sup> Ambrósio et al. attempted to assess the ability of the OCULUS Corvis ST to detect clinical and subclinical ectasia. They concluded that the TBI was accurate for detecting subclinical ectasia among eyes with normal topography in patients with very asymmetric ectasia.<sup>23</sup>

Silverman et al. investigated the epithelial thickness of 12 NPE in patients with very asymmetrical keratoconus using the Artemis very-high-frequency ultrasound epithelial thickness map and found that 33% of the NPE were classified as keratoconus by the Artemis model.<sup>38</sup>

Ayar et al. compared the corneal biomechanical response between 27 patients with unilateral keratoconus and healthy controls using the ORA (CH and CRF). They concluded that the CH and CRF of the NPE showed significant pathological results compared with normal CG.<sup>39</sup>

In this study, the CH and CRF are the only parameters that showed a statistical significance and ability to detect

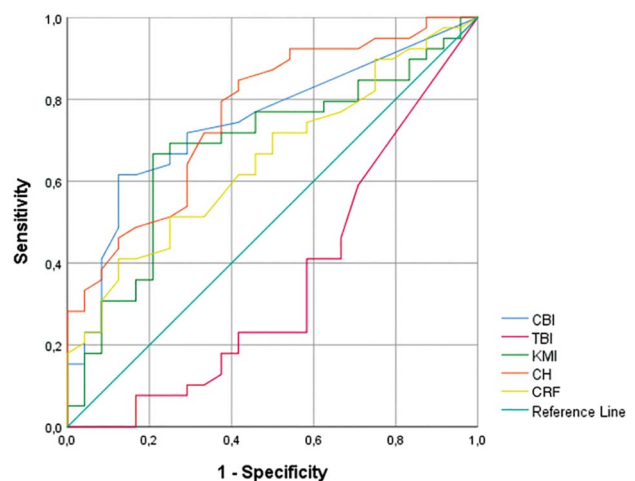


**Figure 5.** ROC curve analysis on the topotomographically NPE for CH, CRF, KMI, TBI, and CBI. Diagonal segments are produced by ties. ROC curves were used to determine the overall predictive accuracy of the CBI, KMI, and TBI to detect abnormalities on the NPE. An area of 1 (100%) implies that the test perfectly discriminates ectatic changes on NPE. The CH showed the best ability to detect ectatic changes with an AUC of 0.74. Only the TBI showed a poor ability to discriminate ectatic changes (AUC < 0.5). However, none of the 4 others parameters differed significantly from each other (AUC = area under the curve; CH = corneal hysteresis; CBI = Corvis biomechanical index; CRF = corneal resistance factor; KMI = keratoconus match index; NPE = topotomographically normal partner eye; ROC = receiver operating characteristic; TBI = topographic biomechanical index).

biomechanical abnormalities on the NPE of patients with very asymmetrical keratoconus. The KMI and TBI did not differ significantly overall. On the contrary, the CBI showed significantly more pathological values for the CG compared with the NPE. However, the ROC curve did not isolate a better parameter to detect early biomechanical changes. Nonetheless, the ROC curve has shown that the TBI is the least efficient for this purpose. These results can be explained by the fact that the TBI combines the Scheimpflug-based corneal tomography with the biomechanical parameters of the Corvis ST.<sup>23</sup>

LASIK is known to alter the corneal biomechanical response, which is an important factor affecting postoperative refractive results. It is critical for refractive surgeons to screen and identify corneas predisposed to develop postoperative complications such as ectasia. In this study, we analyzed the corneal biomechanical response of stable patients who underwent LASIK and concluded that LASIK could complicate the early detection of biomechanical abnormalities, taking into account that LASIK itself induces biomechanical alterations.<sup>40</sup> Therefore, LASIK complicates the differentiation between biomechanical alterations induced by the LASIK itself and biomechanical alterations due to early corneal ectasia. In our study, the CBI seems to be the most efficient parameter to distinguish a NPE from a post-LASIK eye ( $P = .001$ ).

Li et al. tried to determine the rate at which clinically NPE in unilateral keratoconus will progress into keratoconus. They recruited 116 patients with unilateral keratoconus and found that approximately 50% of the NPE progressed into keratoconus within 16 years.<sup>2</sup> This leads us to a single question: does the true unilateral keratoconus exist in the long-term or do these cases eventually progress into a bilateral form?

This study points out the importance of the biomechanical corneal destabilization detectable even before the tomographic and clinical signs of the disease. The early detection of any subclinical or early-stage corneal ectasia such as a keratoconus is very important in the setting of any type of refractive surgery. Unpredictable postoperative results and patient dissatisfaction after refractive surgery have been attributed to the existence of undiagnosed subclinical corneal ectasia and show the importance of preoperative biomechanical screening.

Main potential limitation of our study was the relatively small population from a single medical center. The clinical records of 1730 patients from our Homburg Keratoconus Center were collected and reviewed. Because very asymmetrical ectasia is a rare phenomenon, only 26 patients (1.5%) with very asymmetrical ectasia were detected and recruited into our study. The variability of the single measures causes a statistical bias because of the small patient cohort. This bias was corrected by using statistical formulas for small cohorts (non-Gaussian samples). However, a bigger patient cohort is required to confirm the tendency of our results. A longitudinal analysis for more than 3 to 5 years to study the progression of all the biomechanical parameters and indices is currently investigated by our group to see the evolution and to confirm the tendency of these results. Further studies with larger

cohorts are eventually necessary to confirm our results and further explore the diagnostic potential of these new biomechanical parameters.

Topographically and tomographically very asymmetrical corneal ectasia can show biomechanical changes on the partner eye, which is primarily considered normal. Further investigations, such as the biomechanical response, on the NPE of very asymmetrical ectasia seems to confirm that the truly unilateral keratoconus might be an extremely rare phenomenon. This should be considered before planning any type of refractive corneal surgery.

#### WHAT WAS KNOWN

- Numerous studies have attempted to investigate the diagnostic capacity of devices measuring the corneal biomechanical response, such as the Ocular Response Analyzer (ORA) and Oculus Corvis ST, to detect biomechanical changes on keratoconus-suspect eyes, such as the topotomographically normal partner eye in unilateral keratoconus.
- They concluded that the ORA or Oculus Corvis ST, depending on the study, could help to diagnose early subclinical forms of keratoconus and that the truly unilateral keratoconus does not exist.

#### WHAT THIS PAPER ADDS

- The ORA (corneal hysteresis and corneal resistance factor) showed significant biomechanical abnormalities on the partner eye, which is primarily considered normal in very asymmetric corneal ectasia.
- Compared with the ORA, the Corvis ST seemed to be less sensitive to detect early biomechanical changes in subclinical corneal ectasia. It supported the conclusion that truly unilateral keratoconus does not exist.

#### REFERENCES

1. Gordon-Shaag A, Millodot A, Shneur A. The epidemiology and etiology of keratoconus. *Int J Kerat Ect Cor Dis* 2012;1:7–15
2. Li X, Rabinowitz YS, Rasheed K, Yang H. Longitudinal study of the normal eyes in unilateral keratoconus patients. *Ophthalmology* 2004;111:440–446
3. Galvis V, Sherwin T, Tello A, Merayo J, Barreta R, Acera A. Keratoconus: an inflammatory disorder? *Eye (Lond)* 2015;29:843–859
4. Stachon T, Latta L, Kolev K, Seitz B, Langenbacher A, Szentmáry N. Increased NF- $\kappa$ B and iNOS expression in keratoconus keratocytes-hints for an inflammatory component? [in German]. *Klin Monatsbl Augenheilkd* 2019. doi: 10.1055/a-1002-0100 [Epub ahead of print.]
5. Alió JL. Keratoconus. *Recent Advances in Diagnosis and Treatment*. Switzerland: Springer; 2017:13–23
6. Wang Y, Rabinowitz YS, Rotter JI, Yang H. Genetic epidemiological study of keratoconus: evidence for major gene determination. *Am J Med Genet* 2000;93:403–409
7. Sugar J, Macsai MS. What causes keratoconus? *Cornea* 2012;31:716–719
8. Gomes JAP, Tan D, Rapuano CJ, Belin MW, Ambrósio R, Guell JL, Malecaze F, Nishida K, Sangwan VS; Group of Panelists for the Global Delphi Panel of Keratoconus and Ectatic Diseases. Global consensus on keratoconus and ectatic diseases. *Cornea* 2015;34:359–369
9. Hashemi H, Beiranvand A, Khabazkhoob M, Asgari S, Emamian MH, Shariati M, Fotouhi A. Prevalence of keratoconus in a population-based study in Shahroud. *Cornea* 2013;32:1441–1445
10. Assri AA, Yousuf BI, Quantock AJ, Murphy PJ. Incidence and severity of keratoconus in Asir province Saudi Arabia. *Br J Ophthalmol* 2005;89:1403–1406
11. Gatinel D. Eye rubbing, a sine qua non for keratoconus. *Int J Kerat Ect Cor Dis* 2016;5:6–12
12. Gordon-Shaag A, Millodot M, Shneur E, Liu Y. The genetic and environmental factors for keratoconus. *Biomed Res Int* 2015;2015:738–795

13. Naderan M, Shoar S, Rezagholizadeh F, Zolfaghari M, Naderan M. Characteristics and associations of keratoconus patients. *Cont Lens Anterior Eye* 2015;38:199–205
14. Eppig T, Spira-Eppig C, Goebels S, Seitz B, El-Husseiny M, Lenhart M, Papavasileiou K, Szentmáry N, Langenbucher A. Asymmetry between left and right eyes in keratoconus patients increases with the severity of the worse eye. *Curr Eye Res* 2018;43:848–855
15. Roberts CJ, Dupps WJ, Downs CJ. *Biomechanics of the Eye*. Amsterdam, Netherlands: Kugler Publications; 2018;1:199–203
16. Luz A, Lopes B, Hallahan K, Valbon B, Ramos I, Faria-Correia F, Schor P, Dupps W, Ambrósio R. Enhanced combined tomography and biomechanics data for distinguishing forme fruste keratoconus. *J Cataract Refract Surg* 2016;32:479–494
17. Ramos IC, Reinstein DZ, Archer TJ, Gobbe M, Salomão MQ, Lopes B, Luz A, Faria-Correia F, Gatinel D, Belin MW, Ambrósio R. Unilateral ectasia characterized by advanced diagnostic tests. *Int J Keratoconus Ectatic Dis* 2016;5:40–51
18. Elham R, Jafarzadehpur E, Hashemi H, Amanzadeh K, Shokrollahzadeh F, Yekta A, Khabazkhoob M. Keratoconus diagnosis using Corvis ST measured biomechanical parameters. *J Curr Ophthalmol* 2017;29:175–181
19. Lafond G, Bazin R, Lajoie C. Bilateral severe keratoconus after laser in situ keratomileusis in a patient with forme fruste keratoconus. *J Refract Surg* 2001;27:1115–1118
20. Wang Jim C, Hufnagel T, Buxton DF. Bilateral keratectasia after unilateral laser in situ keratomileusis: a retrospective diagnosis of ectatic corneal disorder. *J Refract Surg* 2003;29:2015–2018
21. Roberts CJ, Mahmoud AM, Bons JP, Hossain A, Elsheikh A, Vinciguerra R, Vinciguerra P, Ambrósio R. Introduction of two novel stiffness parameters and interpretation of air puff-induced biomechanical deformation parameters with a dynamic Scheimpflug analyzer. *J Refract Surg* 2017;33:266–273
22. Lopes BT, Ramos IC, Salomão MQ, Guerra FP, Schallhorn SC, Schallhorn JM, Vinciguerra R, Vinciguerra P, Price FW Jr, Price MO, Reinstein DZ, Archer TJ, Belin MW, Machado AP, Ambrósio R Jr. Enhanced tomographic assessment to detect corneal ectasia based on artificial intelligence. *Am J Ophthalmol* 2018;195:223–232
23. Ambrósio R, Lopes BT, Faria-Correia F, Salomao M, Bühren J, Roberts CJ, Elsheikh A, Vinciguerra R, Vinciguerra P. Integration of Scheimpflug-based corneal tomography and biomechanical assessments for enhancing ectasia detection. *J Cataract Refract Surg* 2017;33:434–444
24. Fontes BM, Ambrósio R, Velarde GC, Nosé W. Ocular response analyzer measurements in keratoconus with normal central corneal thickness compared with matched normal control eyes. *J Refract Surg* 2011;27:209–215
25. Vinciguerra R, Ambrósio R, Elsheikh A, Roberts CJ, Lopes B, Morengi E, Azzolini C, Vinciguerra P. Detection of keratoconus with a new biomechanical index. *J Refract Surg* 2016;32:803–810
26. Belin MW, Khachikian SS. Keratoconus/ectasia detection with the oculus pentacam: Belin/Ambrósio enhanced ectasia display. *Highlights Ophthalmol* 2007;35:5–12
27. Cui J, Zhang X, Hu Q, Zhou WY, Yang F. Evaluation of corneal thickness and volume parameters of subclinical keratoconus using a pentacam Scheimpflug system. *Curr Eye Res* 2016;41:923–926
28. Rabinowitz YS, McDonnell PJ. Computer-assisted corneal topography in keratoconus. *J Refract Surg* 1989;5:400–408
29. Huseynli S, Abdulaliyeva F. Evaluation of Scheimpflug Tomography parameters in subclinical keratoconus, clinical keratoconus and normal Caucasian Eyes. *Turk J Ophthalmol* 2018;48:99–108
30. Chan TC, Wang YM, Yu M, Jhanji V. Comparison of corneal dynamic parameters and tomographic measurements using Scheimpflug imaging in keratoconus. *Br J Ophthalmol* 2018;102:42–47
31. Cohen J. *Statistical Power Analysis for the Behavioral Sciences*. Mahwah, NJ: Lawrence Erlbaum Associates; 1988;20–27
32. Goebels S, Eppig T, Wagenpfeil S, Cayless A, Seitz B, Langenbucher A. Staging of keratoconus indices regarding tomography, topography, and biomechanical measurements. *Am J Ophthalmol* 2015;159:733–738
33. Shah S, Laiquzzaman M, Bhojwani R, Mantry S, Cunliffe I. Assessment of biomechanical properties of the cornea with the ocular response analyzer in normal and keratoconic eyes. *Invest Ophthalmol Vis Sci* 2007;48:3026–3031
34. Labiris G, Giarmoukakis A, Gatziofias Z, Sideroudi H, Kozobolis V, Seitz B. Diagnostic capacity of the keratoconus match index and keratoconus match probability in subclinical keratoconus. *J Cataract Refract Surg* 2014;40:999–1005
35. Luce DA. Determining in vivo biomechanical properties of the cornea with an ocular response analyzer. *J Cataract Refract Surg* 2005;31:156–162
36. Luz A, Fontes B, Ramos IC, Lopes B, Correia F, Schor P, Ambrósio R. Evaluation of ocular biomechanical indices to distinguish normal from keratoconus eyes. *Int J Kerat Ect Cor Dis* 2012;1:145–150
37. Vinciguerra R, Ambrósio R, Roberts CJ, Azzolini C, Vinciguerra P. Biomechanical characterization of subclinical keratoconus without topographic or tomographic abnormalities. *J Refract Surg* 2017;33:399–407
38. Silverman RH, Urs R, Archer TJ, Gobbe M, Reinstein DZ. Assessment of contralateral eye in unilateral keratoconus using artemis epithelial maps. *Invest Ophthalmol Vis Sci* 2015;56:1617
39. Ayar O, Ozmen MC, Muftuoglu O, Akdemir MO, Koc M, Ozulken K. In-vivo corneal biomechanical analysis of unilateral keratoconus. *Int J Ophthalmol* 2015;8:1141
40. Ortiz D, Piñero D, Shabayek MH, Arnalich-Montiel F, Alió JL. Corneal biomechanical properties in normal, post-laser in situ keratomileusis, and keratoconic eyes. *J Cataract Refract Surg* 2007;33:1371–1375

**Disclosures:** *None of the authors has a financial or proprietary interest in any material or method mentioned.*